Ocean acidification impacts bacteria-phytoplankton coupling at low nutrient-conditions

Thomas Hornick[1], Lennart T. Bach[2], Katharine J. Crawfurd[3], Kristian Spilling[4,5], Eric P. Achterberg[2,6], Jason N. Woodhouse[1], Kai G. Schulz[2,7], Corina P. D. Brussaard[3,8,], Ulf Riebesell[2], Hans-Peter Grossart[1,9]

[1]{Leibniz Institute of Freshwater Ecology and Inland Fisheries (IGB), Experimental Limnology, 16775 Stechlin, Germany}

[2]{GEOMAR Helmholtz Centre for Ocean Research Kiel, Düsternbrooker Weg 20, 24105 Kiel, Germany}

[3]{ NIOZ Royal Netherlands Institute for Sea Research, Department of Marine Microbiology and Biogeochemistry, and Utrecht University, P.O. Box 59, 1790 AB Den Burg, Texel, The Netherlands}

[4]{Marine Research Centre, Finnish Environment Institute, P.O. Box 140, 00251 Helsinki, Finland}

[5]{Tvärminne Zoological Station, University of Helsinki, J. A. Palménin tie 260, 10900 Hanko, Finland}

[6]{National Oceanography Centre Southampton, European Way, University of Southampton, Southampton, SO14 3ZH, UK}

[7]{Southern Cross University, P.O. Box 157, Lismore, NSW 2480, Australia}

[8]{Aquatic Microbiology, Institute for Biodiversity and Ecosystem Dynamics, University of Amsterdam, P.O. Box 94248, 1090 GE Amsterdam, The Netherlands}

[9]{Potsdam University, Institute for Biochemistry and Biology, 14469 Potsdam, Maulbeerallee 2, Germany}

Correspondence to: T. Hornick (hornick@igb-berlin.de)

Abstract

The oceans absorb about a quarter of the yearly produced anthropogenic atmospheric carbon dioxide (CO_2), resulting in a decrease in surface water pH, a process termed ocean acidification (OA). Surprisingly little is known about how OA affects the physiology of heterotrophic bacteria or the coupling of heterotrophic bacteria to phytoplankton when nutrients are limited. Previous experiments were, for the most part, undertaken during productive phases or following nutrient additions designed to stimulate algal blooms. Therefore, we undertook an *in situ* large-volume mesocosm (~55 m^3) experiment in the Baltic Sea by simulating different fugacities of CO_2 (fCO_2) extending from present to future conditions. The study was conducted in July-August after the nominal spring-bloom, in order to maintain low-nutrient conditions throughout the experiment. This resulted in phytoplankton communities dominated by small-sized functional groups (picophytoplankton). There was no consistent fCO_2-induced effect on bacterial protein production (BPP), cell-specific BPP (csBPP) or biovolumes (BVs) of either FL or PA heterotrophic bacteria, when considered as individual components (univariate analyses). Permutational Multivariate Analysis of Variance (PERMANOVA) revealed a significant effect of the fCO_2-treatment on entire assemblages of dissolved and particulate nutrients, metabolic parameters and the bacteria-phytoplankton community. However, distance-based linear modelling only identified fCO_2 as a factor explaining the variability observed amongst the microbial community composition, but not for explaining variability within the metabolic parameters. This suggests that fCO_2 impacts on microbial metabolic parameters occurred indirectly through varying physiochemical parameters and microbial species composition. Cluster analyses examining the co-occurrence of different functional groups of bacteria and phytoplankton further revealed a separation of the four fCO_2-treated mesocosms from both control mesocosms, indicating that complex trophic interactions might be altered in a future acidified ocean. Possible consequences for nutrient cycling and carbon export are still largely unknown, in particular in a nutrient limited ocean.

Key words

Ocean acidification, CO_2 enrichment, trophic interaction, Baltic Sea, KOSMOS mesocosm experiment, bacterial production, phytoplankton

1 Introduction

Since the industrial revolution the oceans have absorbed ca. one half of the anthropogenic carbon dioxide (CO_2). This has resulted in a shift in carbonate equilibria and pH (e.g. Caldeira and Wickett, 2003) with potential consequences for organismal physiology (Taylor et al., 2012). In principal, autotrophs should be fertilized by an enhanced CO_2 availability, increasing the production of particulate (POM) and dissolved organic matter (DOM) (Hein and Sand-Jensen, 1997; Riebesell et al., 2007). However, most CO_2 enrichment experiments studying natural plankton assemblages under variable nutrient conditions do not reveal a consistent response of primary production to elevated CO_2 (e.g. Engel, et al., 2005; Riebesell et al., 2007; Bach et al., 2016). Both amount and stoichiometric composition of algal DOM and POM can be affected by changes in fCO_2. For example, Riebesell et al. (2007) and Maat et al. (2014) reported an increased stoichiometric drawdown of carbon (C) to nitrogen (N) at higher levels of fCO_2, most likely as a result from C-overconsumption (Toggweiler, 1993).

Heterotrophic bacteria, in oligotrophic systems, are largely dependent on phytoplankton derived organic carbon (e.g. Azam, 1998), and as such respond to alterations in both the quantity and quality of phyotplankton derived DOM and POM (e.g. Allgaier et al., 2008; Grossart et al., 2006a). Availability and competition for nutrients, however, can substantially impact fCO_2-induced changes in activity and biomass of phytoplankton and subsequently of heterotrophic bacteria. In nutrient-depleted or nutrient-limited systems, bacteria are restricted in their utilization of phytoplankton derived organic carbon (Hoikkala et al., 2009; Lignell et al., 2008). Consequently, fCO_2 dependent increases in inorganic C-availability for autotrophs may not stimulate heterotrophic activity, causing a decoupling of heterotrophic and autotrophic processes (Thingstad et al., 2008). The accumulation of bioavailable dissolved organic carbon (DOC) and particulate organic carbon (POC), as a consequence of this decoupling in nutrient limited oceanic surface waters, may have profound consequences for nutrient cycling and the nature of the oceanic carbon pump (e.g. Thingstad et al., 1997). Given that various studies have reported on limitation of bacterial growth by inorganic nutrients in several parts of the Baltic Sea (e.g. Hoikkala et al., 2009; Kuparinen and Heinänen, 1993), we sought to evaluate the effects of enhanced fCO_2 on activity and biomass of free-living (FL) as well as particle associated (PA) bacteria during a period characterised by low nutrients and low productivity.

2 Methods

2.1 Experimental setup, CO_2 manipulation and sampling

Nine floating, pelagic KOSMOS (Kiel Off-Shore Mesocosms for future Ocean Simulations) mesocosms (cylindrical, 2 m diameter, 17 m long with conical sediment trap extending to 19 m depth) were moored on 12th June 2012 (day -10 = t-10; 10 days before CO_2 manipulation) at 59°51.5´N, 23°15.5'E in the Baltic Sea at Tvärminne Storfjärden on the south-west coast of Finland. Exposed mesocosm bags were rinsed for a period of five days, covered on the top and bottom with a 3 mm net to exclude larger organisms. Thereby, the containing water was fully exchanged with the surrounding water masses. Five days prior the start of the experiment (t-5), sediment traps were attached to the bottom of each mesocosm at 17 m depth. In addition, submerged mesocosm bags were drawn 1.5 m above the water surface, enclosing and separating ~55 m^3 of water from the surrounding Baltic Sea and meshes were removed. Mesocosms were covered by a photosynthetic active radiation (PAR) transparent roof to prevent nutrient addition from birds and freshwater input from rain. Additionally, existing haloclines were removed in each mesocosm as described in Paul et al. (2015), thereby creating a fully homogeneous water body.

The experiment was conducted between 17th June (t-5) and 4th August (t43) 2012. To minimize environmental stress on enclosed organisms CO_2 addition was performed stepwise over three days commencing on day t0. CO_2 addition was repeated at t15 in the upper mixed 7 m to compensate for outgassing. Different fCO_2 treatments were achieved by equally distributing filtered (50 µm), CO_2-saturated seawater into the treated mesocosms with a water distributor as described by Paul et al. (2015). Control mesocosms were also manipulated with the water distributor and 50 µM pre-filtered water without CO_2. CO_2 amendments resulted in ca. 0.04-0.35 % increases in the total water volume across mesocosms (Paul et al. 2015). Integrated water samples (0-17 m) were collected from each mesocosm and the surrounding seawater using depth-integrated water samplers (IWS, HYDRO-BIOS, Kiel). Samples for activity measurements were directly subsampled from the IWS on the sampling boat without headspace to maintain in-situ fCO_2 concentrations during incubation.

Unfortunately, three mesocosms failed during the experiment, as a consequence of welding faults, resulting in unquantifiable water exchanges with the surrounding waters. Therefore, with reference to the six remaining mesocosms, CO_2 concentrations defining each treatment are reported as the mean fCO_2 concentration determined over the initial 43 days (t1-t43) as described in Paul et al. (2015). The control mesocosms (two replicates) had 365 µatm and 368 µatm fCO_2, respectively. The four treatment mesocosms each had 497 µatm, 821 µatm, 1007 µatm and 1231 µatm fCO_2, respectively. Detailed descriptions on the study site, mesocosm deployment and system, performance of the mesocosm facility throughout the experiment, CO_2 addition, carbonate chemistry, cleaning of the mesocosm bags as well as sampling frequencies of single parameters are given in Paul et al. (2015).

2.2 Physical and chemical parameters

Physical measurements (i.e. temperature and salinity) were performed using a CTC60M memory probe (Sea and Sun Technology, Trappenkamp, Germany) and are calculated as the mean, integrated over the total depth. Photosythetic active radiation (PAR) was measured with a PAR sensor (LI-COR LI-192) at the roof of Tvärminne Zoological Station.

Samples for dissolved inorganic carbon concentrations (DIC) and total pH were gently pressure-filtered (Sarstedt Filtropur PES, 0.2 µm pore size) using a membrane pump (Stepdos). Total pH was determined as described in Dickson et al. (2007) on a Cary 100 (Varian) spectrophotometer in a temperature-controlled 10 cm cuvette using a *m*-cresol indicator dye. DIC concentrations were determined by infrared absorption using a LI-COR LI-7000 on an AIRICA system (MARIANDA, Kiel). Total pH and DIC were used to calculate carbonate chemistry speciation using the stoichiometric equilibrium constants for carbonic acid of Mehrbach et al. (1973) as refitted by Lueker et al. (2000).

Samples for dissolved organic carbon (DOC), total dissolved nitrogen (TDN) as well as dissolved silica (DSi) and dissolved inorganic phosphate (DIP) were filtered through pre-combusted (450 °C, 6h) GF/F filters (Whatman, nominal pore size of 0.7 µm). Concentrations of DOC and TDN were determined using a high-temperature catalytic combustion technique with a Shimadzu TOC-TN V analyser following Badr et al. (2003). DSi concentrations were determined using standard colorimetric techniques (Grasshoff et al. 1983) at the micromolar level with a nutrient autoanalyser (Seal Analytical, Quattro). DIP concentrations were

149 determined with a colorimetric method using a 2 m liquid waveguide capillary cell (Patey et
150 al., 2008) with a miniaturised detector (Ocean Optics Ltd).

151 Total particulate carbon (TPC), particulate organic nitrogen (PON) and total particulate
152 phosphorus (TPP) samples were collected onto pre-combusted (450 °C, 6h) GF/F filters
153 (Whatman, nominal pore size of 0.7 µm) using gentle vacuum filtration and stored in glass
154 Petri dishes at -20 ^{o}C. Biogenic silica (BSi) samples were collected on cellulose acetate filters
155 (0.65 µm, Whatman) using gentle vacuum filtration (< 200 mbar) and stored in glass Petri
156 dishes at -20 °C. Filters for TPC/PON analyses were dried at 60 °C, packed into tin capsules
157 and measured on an elemental analyser (EuroEA) according to Sharp (1974), coupled by
158 either a Conflo II to a Finnigan Delta^{Plus} isotope ratio mass spectrometer or a Conflo III to a
159 Thermo Finnigan Delta^{Plus} XP isotope ratio mass spectrometer. Filters for TPP were treated
160 with oxidizing decomposition reagent (MERCK, catalogue no. 112936) to oxidise organic
161 phosphorus to orthophosphate. Particulate silica was leached from filtered material.
162 Concentrations of dissolved inorganic phosphate as well as dissolved silica were determined
163 spectrophotometrically according to Hansen and Koroleff (1999).

164 Samples for chlorophyll *a* (Chl *a*) were filtered on GF/F filters (Whatman, nominal pore size
165 of 0.7 µm) and stored at -20 °C. Chl *a* was extracted in acetone (90 %) and samples
166 homogenized. After centrifugation (10 min, 800 x g, 4 °C) the supernatand was analysed on a
167 fluorometer (TURNER 10-AU) to determine concentrations of Chl *a* (Welschmeyer, 1994).

168 Further details on the determination of physical parameters, concentration of Chl *a* as well as
169 dissolved and particulate nutrients can be obtained from Paul et al. (2015).

170 ## 2.3 Microbial standing stock

171 Abundance of free-living (FL) heterotrophic prokaryotes (HP) and photoautotrophic
172 prokaryotic (*Synechococcus* spp.) as well as eukaryotic cells (<20 µm) were determined by
173 flow cytometry (Crawfurd et al. 2016). Briefly, phytoplankton were discriminated based on
174 their chlorophyll red autofluorescence and/or phycoerythrin orange autofluorescence (Marie
175 et al., 1999). In combination with their side scatter signal and size fractionation the
176 phytoplankton community could be divided into 6 clusters, varying in size from 1 to 8.8 µm
177 average cell diameter (Crawfurd et al., 2016). Three groups of picoeukaryotic phytoplankton
178 (Pico I-III), 1 picoprokaryotic photoautotroph (*Synechococcus* spp.) and 2 nanoeukaryotic

phytoplankton groups were detected. Biovolume (BV) estimations were based on cell abundance and average cell diameters by assuming a spherical cell shape. The BV sum of Synechococcus and Pico I-III is expressed as BV_{Pico}. The BV sum of Nano I and II will be referred as BV_{Nano}.

Abundances of FL prokaryotes were determined from 0.5 % glutaraldehyde fixed samples after staining with the nucleic acid-specific dye SYBR green I (Crawfurd et al. 2016). Unicellular cyanobacteria (*Synechococcus* spp.) contributed maximally 10% of the total counts. Two additional groups were identified based on their low (LDNA) and high (HDNA) fluorescence. This identification was based on gating of SYBR green I fluorescence against the side scatter signal (Crawfurd et al., 2016). Particle-associated (PA) prokaryotes were enumerated by epifluorescence-microscopy on a Leica Leitz DMRB fluorescence microscope with UV- and blue light excitation filters (Leica Microsystems, Wetzlar, Germany). Fresh samples were gently mixed to prevent particle settling and a 15 mL subsample was filtered on a 0.1-% Irgalan Black coloured 5.0 µm polycarbonate-filter (Whatman, Maidstone, UK) (Hobbie et al., 1977). Filters were fixed with glutaraldehyde (Carl Roth, Karlsruhe, Germany, final conc. 2 %) and stained for 15 min with 4´6-diamidino-2-phenylindole (DAPI, final conc. 1 µg mL^{-1}) (Porter and Feig, 1980) directly on the filtration device and rinsed twice with sterile filtered habitat water before air-drying and embedding in Citifluor AF1 (Citifluor Ltd, London, UK) on a microscopic slide (Rieck et al., 2015). Counts were made based on 15 random unique squares as observed at a magnification of 1000x. The total number of heterotrophic PA prokaryotes was enumerated by subtracting Chl *a* autofluorescent cells from DAPI-stained cells (Rieck et al., 2015).

BV of FL and PA prokaryotes were calculated separately. For FL prokaryotes we estimated BVs on the basis of an average cell volume of 0.06 μm^3 (Hagström et al., 1979). BV of PA prokaryotes were calculated from measurements of 1600 cells across 3 different mesocosms (346 µatm, 868 µatm, 1333 µatm) and three time points (t0, t20, t39) throughout the experiment (Massana et al., 1997). A resulting average BV of 0.16 μm^3 per cell was used to calculate BV of PA prokaryotes derived from cell abundances. We subsequently adopted the term “heterotrophic bacteria”, since bacteria account for the majority of non- photosynthetic prokaryotes in surface waters (Kirchman et al. 2007).

2.4 Metabolic parameters

Rates of bacterial protein production (BPP) were determined by incorporation of ^{14}[C]-leucine (^{14}C-Leu, Simon and Azam, 1989) according to Grossart et al. (2006a). Triplicates and a formalin-killed control were incubated with ^{14}C-Leu (213 mCi mmol^{-1}; Hartmann Analytic GmbH, Germany) at a final concentration of 165 nM, which ensured saturation of the uptake systems of both FL and PA bacteria. Incubation was performed in the dark at *in situ* temperature (between 7.8 °C and 15.8 °C) for 1.5 h. After fixation with 2% formalin, samples were filtered onto 5.0 µm (PA bacteria) nitrocellulose filters (Sartorius, Germany) and extracted with ice-cold 5% trichloroacetic acid (TCA) for 5 min. Thereafter, filters were rinsed twice with ice-cold 5% TCA, once with ethanol (50% v/v), and dissolved in ethylacetate for measurement by liquid scintillation counting (Wallac 1414, Perkin Elmer). Afterwards, the collected filtrate was filtered on 0.2 µm (FL bacteria) nitrocellulose filters (Sartorius, Germany) and processed in the same way as the 5.0 µm filters. Standard deviation of triplicate measurements was usually <15%. The amount of incorporated ^{14}C-Leu was converted into BPP by using an intracellular isotope dilution factor of 2. A conversion factor of 0.86 was used to convert the produced protein into carbon (Simon and Azam, 1989). Cell-specific BPP rates (csBPP) were calculated by dividing BPP-rates by abundances of FL prokaryotes and PA HP.

Community respiration (CR) rates were calculated from oxygen consumption during an incubation period of 48 hours at *in situ* temperature in the dark by assuming a respiratory quotient of 1 (Berggren et al., 2012). Thereby oxygen concentrations were measured in triplicate in 120 mL O_2 bottles without headspace, using a fiber optical dipping probe (PreSens, Fibox 3), which was calibrated against anoxic and air saturated water.

Primary production (PP) was measured using radio-labeled $NaH^{14}CO_3$ (Steeman-Nielsen, 1952) from 0-10 m depth integrated samples. After incubation of duplicate samples with 10 µL of ^{14}C bicarbonate solution (DHI Lab, 20 µCi mL^{-1}) in 8 mL vials at 2,4,6, 8 and 10 m for 24 h, samples were acidified with 1 M HCl to remove remaining inorganic ^{14}C. Radioactivity was determined by using a scintillation counter (Wallac 1414, Perkin Elmer). PP was calculated knowing the dark-control corrected ^{14}C incorporation and the fraction of the ^{14}C addition to the total inorganic carbon pool according to Gargas (1975). Further details on the measurement of CR and PP are given by Spilling et al. (2016a).

2.5 Statistical analyses

Permutational multivariate analysis of variance – PERMANOVA (Anderson, 2001) was used to determine associations between physical/chemical variables and biotic variables. PERMANOVA (perm=9999) was performed to test for significant differences in variance over time and between *f*CO_2-treated mesocosms (Anderson et al., 2008). Environmental data were normalized according Clarke and Gorley (2006). Biotic abundance data were log(x+1) transformed (Clarke and Gorley, 2006). PERMANOVA partitions the total sum of squares based on the experimental design and calculates a distance based pseudo-*F* statistic for each term in the model. Distance-based linear modeling (DistLM) was implemented to relate physical/chemical predictor variables and the multivariate assemblage of biotic variables (Supplementary Table S1) (Legendre and Anderson, 1999; Anderson et al., 2008). The DistLM routine was based on the AIC model selection criterion (see Anderson et al., 2008) using a step-wise selection procedure. In case of equally AIC-ranked models (difference <1), a model with fewer parameters was preferred. A Principal Component Analysis (PCA) was performed on normalized chemical data to identify chemical gradients and patterns between the differently *f*CO_2-treated mesocosms over time (Clarke and Gorley, 2006). Distance based redundancy analysis (dbRDA) was used for visual interpretation of the DistLM in multi-dimensional space (Anderson et al., 2008). Multivariate analyses of physicochemical, metabolic and community data were performed on a reduced data set comprising 10 time points (t5-t29, every 3rd day, t31), containing all measured activity variables (BPP, areal PP and CR). Missing values of nutrient data or abundance data (based on every other day measurements) were estimated as means of the preceding and following measurement day. No activity data was interpolated or data extrapolated in general.

Cluster analyses were performed based on Spearman´s rank correlation coefficients calculated for each mesocosm between all possible combinations of LDNA, HDNA, pico- and nanophytoplankton abundances as well as total Chl *a*. Thereafter, *p*-values were corrected for multiple testing according Benjamini and Hochberg (1995). The R-package pvclust was used to assess the uncertainty in hierarchical cluster analysis (Suzuki and Shimodeira, 2015). For each cluster, AU (approximately unbiased) *p*-values (between 0 and 1) were calculated via multiscale bootstrap resampling (Suzuki and Shimodaira, 2015).

PERMANOVA, distLM and dbRDA were carried out using Primer 6.0 and PERMANOVA + for PRIMER software (Clarke and Gorley, 2006, Anderson et al., 2008). All other analysis, including PCA and the visualisation of result was performed with R 3.2.5 (R Core Team, 2016) using packages Hmisc (Harrell et al., 2016), vegan (Oksanen et al., 2016), pvclust (Suzuki and Shimodeira, 2015), gplots (Warnes et al., 2016) and ggplot2 (Wickham, 2009).

3 Results

3.1 Bacterial dynamics

Heterotrophic bacterial BV was comprised predominantly of FL bacteria. PA bacteria contributed maximally $2 \pm 0.7 - 10 \pm 0.7$ % (mean 4.8 ± 0.6 %) of total bacterial BV. PA bacteria, however, accounted for a substantial fraction of overall BPP ($27 \pm 1 - 59 \pm 7$ %, mean 39 ± 4 %). There was no significant effect of fCO_2 on BPP, csBPP or BV of neither FL nor PA heterotrophic bacteria ($p_{perm} > 0.05$), however a significant temporal effect was observed ($p_{perm} < 0.05$). Both bacterial size-fractions had distinct dynamics in abundance, BPP and csBPP during the course of the experiment. BPP and bacterial abundances were closely related to Chl *a* and BV of nano- and picophytoplankton, trending along with Chl *a* until t10 and then continuing to increase with BVs of nanophotoautotrophs and Chl *a.* The period between t16 and t26, following a sharp decrease in Chl *a* at t16 revealed highest BPP rates across the experiment with lower rates at higher fCO_2 for PA as well as FL bacteria. CsBPP-rates were lower at elevated fCO_2 for only the FL bacteria during this period. Additionally, BVs of FL and PA bacterial revealed contrasting dynamics (Fig. 1, Fig. S1). PA bacterial BVs declined with the decay of Chl *a*, whereas FL BVs increased strongly associated with an increase in BV of picophotoautotrophs during this period. The ratio of HDNA:LDNA prokaryotes, which both making up FL bacteria, showed also differences between the experimental treatments. Between t14-t25 the ratio of HDNA:LDNA was lower at higher fCO_2.

3.2 Phytoplankton dynamics

Chl *a* concentration exhibited distinct maxima at two time periods (t5 and t16). The second maximum was associated with an increase in the BV of nanophotoautotrophs (BV_{Nano}) (Fig.

2). This increase was reduced in mesocosms containing higher concentrations of fCO_2 between t13-t17. The differences in BV_{Nano} between the treatments were reflected in lower concentrations of Chl *a* in the 3 highest fCO_2-treated mesososms at t16. Chl *a* and BV_{Nano} concentrations declined after t16. In contrast, BV of picophotoautotrophs (BV_{Pico}) increased after t11, associated with an increase in BV of *Synechococcus* spp., which accounted for 31 ± 2 % to 59 ± 2 % of BV_{Pico} across the period of this study (Fig. S2). All four groups of picoautotrophs distinguished by flow cytometry, exhibited time-dependent positive or negative relationships with fCO_2 (Fig. 3, Fig. S2, Fig. S3). The Pico I (~1 µm) and Pico II taxa infrequently exhibited strong fertilization effects in response to the fCO_2-treatment. In contrast, *Synechococcus* spp. and Pico III were infrequently negatively affected by the fCO_2-treatment.

3.3 Relation between functional heterotrophic and autotrophic groups

A cluster analysis of pairwise Spearman correlations between functional bacterial and phytoplankton groups revealed a separation based on fCO_2-treatment. Specifically the four CO_2 amended mesocosms were readily distinguishable from the control treatments. Multiple bootstrap resampling (Suzuki and Shimodaira, 2015) supported this, but only significantly for the three highest fCO_2-treated mesocosms. The two highest fCO_2-treatments revealed a positive correlation of LDNA bacteria and Pico I, which could not be observed in any other experimental treatment. In all CO_2-treated mesocosm we observed positive correlations between *Synechococcus* spp. and Pico III as well as *Synechococcus* spp. and Pico I, which were not present in both control mesocosms. In contrast positive correlations between LDNA and HDNA were not detected in any fCO_2-treatement. Additionally positive correlations between Pico and Nano II as well as HDNA and Cyanobacteria were only present in both controls and the lowest fCO_2-treatment (Fig. 4).

After t10, the ratio between heterotrophic prokaryotic BV and Chl *a* varied between the fCO_2-treatments, but did not show a consistent pattern. After t17, however, the control mesocosms revealed a higher ratio compared to all fCO_2-treated mesocosms (Fig. 5).

3.4 Multivariate physicochemical characterisation

Integrated water temperature and PAR ranged between 8.0 - 15.9 °C and 11.2 - 66.8 mol m^{-2} day^{-1} during the experiment, respectively. Integrated water temperature reached the maximum at t15 and dropped again to 8.2 °C at t31.

PERMANOVA results (Table 1) on a multivariate assemblage of dissolved (DOC, TDN, Phosphate, BSi) and particulate (TPC, PON, POP, BSi) nutrients showed significant temporal (Time-$F_{9,10}$=11.1, p=0.0001) and spatial variations along the fCO_2-gradient (fCO_2-$F_{4,10}$=2.6, p=0.02). PCA ordination of the same chemical dataset strongly reflects the temporal pattern, separating the initial time points before t11 from other time points of the experiments along the first PCA axis (Fig. 6). Thereby, Eigenvectors of TPC and PON loaded highest on PCA axis 1 (Table 2). PCA axis two was mainly characterized by high eigenvectors of dissolved phosphate as well as dissolved and particulate silica. The first two PCA axes explained 69 % of variation and cumulatively 80% with including axis three (Table 2).

3.5 Multivariate characterisation of metabolic parameters

PERMANOVA on the resemblance matrix of normalized metabolic variables (BPP, areal PP, CR) revealed significant temporal (Time-$F_{9,10}$=6.7, p=0.0002) and spatial variations along the fCO_2-gradient (fCO_2-$F_{4,10}$=2.64, p<0.03) (Table 3). DistLM identified significant effects of temperature (p<0.03), phosphate (p<0.02), DOC (p<0.05) and BSi (p<0.02) on the multivariate assemblage of metabolic variables (Table 4). The step-wise procedure selects PAR, temperature, DOC and phosphate as determining factors (AIC=59.6; R^2=0.26; number of variables=4). The dbRDA ordination separates the temporal development. Thereby, 92 % of the variability in the fitted model and 24 % of the total variation is explained by the first two dbRDA axes (Fig. 6).

3.6 Multivariate characterisation of the bacterioplankton and phytoplankton community

PERMANOVA on the resemblance matrix of a multivariate assemblage comprising variables of bacterial and phytoplankton communities (abundances of Pico I-III, Nano I-II, FL bacteria (HDNA, LDNA), PA bacteria, *Synechococcus* spp. and Chl *a*) revealed significant temporal (Time-$F_{9,10}$=56.8, p=0.0001) and spatial variations along the fCO_2-gradient (fCO_2-$F_{4,10}$=14.9,

p=0.0001) (Table 5). DistLM identified significant effects of fCO_2 (p<0.02), temperature (p<0.001), phosphate (p<0.003), TPC (p<0.001), BSi (p<0.001) and POP (p<0.001) on the multivariate assemblage of bacterial and phytoplankton communities (Table 6). The step-wise procedure selects fCO_2, temperature, TPC and phosphate as determining factors (AIC=67.2; R^2=0.44; number of variables=4). The dbRDA reveals a separation along the gradient of fCO_2 on the second dbRDA axis. The first dbRDA axis represents the overall temporal development. Thereby the first two dbRDA axes capture 74 % of the variability in the fitted model and 32 % of the total variation.

4 Discussion

Although OA and its ecological consequences have received growing recognition during the last decade (Riebesell and Gattuso, 2015), surprisingly little is known about the ecological effects on heterotrophic bacterial biomass, production or the coupling of bacterio- and phytoplankton at nutrient limited conditions. Previous experiments were, for the most part, conducted during productive phases of the year (e.g. phytoplankton blooms), under eutrophic conditions (e.g. coastal areas) or with nutrient additions (e.g. Grossart et al., 2006a; Allgaier et al., 2008; Brussaard et al., 2013; Bach et al, 2016). However, large parts of the oceans are nutrient-limited or experience extended nutrient-limited periods during the year (Moore et al., 2013). Thus, we conducted our experiment in July-August, when nutrients and phytoplankton production were relatively low in the northeastern Baltic Sea (Hoikkala et al., 2009; Lignell et al., 2008) and exposed a natural plankton community to different levels of CO_2.

4.1 Phytoplankton-bacterioplankton coupling at low nutrient conditions

Heterotrophic bacteria are important recyclers of autochtonous DOM in aquatic systems and play an important role in nutrient remineralisation in natural plankton assemblages (Kirchman 1994). BV and production of heterotrophic bacteria are highly dependent on quantity and quality of phytoplankton-derived organic carbon and usually are tightly related to phytoplankton development (e.g. Grossart et al., 2006b; Allgaier et al., 2008). During this study, low nitrogen availability limited overall autotrophic production (Paul et al., 2015; Nausch et al., 2016). This resulted in a post spring bloom phytoplankton community, dominated by picophytoplankton (Paul et al., 2015). This is consistent with previous reports

of picophytoplankton accounting for a large fraction of total phytoplankton biomass in oligotrophic, nutrient poor systems (e.g. Agawin et al., 2000). Chl *a* dynamics indicated two minor blooms of larger phytoplankton during the first half of the experiment, although picophytoplankton still accounted for mostly >50 % of the total Chl *a* during this period (Paul et al., 2015; Spilling et al., 2016b). The phytoplankton development was also reflected in the PCA ordination of dissolved and particulate nutrients, clearly separating the preceding period before t11, including the first peak of Chl *a*, from the other observations during the experiment on principal component 1 (Fig. 6). The separation was primarily driven by concentrations of particulate matter (Table 2), which decreased until t11 and subsequently sank out of the water column (Paul et al., 2015).

Bacterial BV and BPP paralleled phytoplankton development during this period. With the decay of the initial phytoplankton bloom, a second bloom event resulted, comprised primarily of nanophytoplankton and picophytoplankton (Crawfurd et al., 2016). A decrease in nanophytoplankton BV and Chl *a* concentrations after t16/t17 benefitted both FL heterotrophic bacteria and picophotoautotrophs. The increased availability of DOM, resulting from cell lysis and remineralisation of POM was associated with increases in the BV of both groups and bacterial production levels (Fig. 1, Fi. S1). We attributed these increases to the cells of Picoplankton which, due to their high volume to surface ratio as well as a small boundary layer surrounding these cells, are generally favoured compared to larger cells in terms of resource acquisition at low nutrient conditions (Raven, 1998; Moore et al., 2013). If cell size is the major factor determining the access to dissolved nitrogen and phosphorous, bacteria should be able to compete equally or better with picophytoplankton at low concentrations (Suttle et al., 1990; Drakare et al., 2003). However, when phytoplankton is restricted in growth due to the lack of mineral nutrients, a strong comensalistic relationship between phytoplanktonic DOM production and bacterioplanktonic DOM utilization may evolve (Azam et al., 1983; Bratbak and Thingstad, 1985; Joint et al., 2002). Although heterotrophic microbes may indirectly limit primary production by depriving phytoplankton of nutrients, they would not be able to outcompete autotrophs completely since this would remove their source of substrates for carbon and energy (Bratbak and Thingstad, 1985; Joint et al., 2002). Such a relationship might explain the paralleled increase in FL bacterial and picophytoplankton BV.

PA bacteria are typically impacted to a lesser extent by nutrient limitation due to consistently higher nutrient availability at particle surfaces (e.g. Grossart and Simon, 1993). This was reflected in this study by the maintenance of high csBPP rates associated with PA heterotrophic bacteria throughout the whole experiment. Overall, PA bacteria contributed only a minor fraction (maximal 10 ± 0.7 %) to the overall bacterial BV, which is typical for oligotrophic or mesotrophic ecosystems (Lapoussière et al., 2010). Nevertheless, their substantial contribution to overall BPP emphasizes their importance, especially during such low productive periods (e.g. Grossart, 2010). PA heterotrophic bacteria are essential for the remineralization of nutrients from autotrophic biomass, which would otherwise sink out from surface waters (Grossart, 2010). Leakage of hydrolysis products and the attachment and detachment of bacteria to and from particles stimulate production amongst free-living bacteria (Smith et al., 1992; Grossart 2010) and picophytoplankton.

4.2 Effects of fCO_2/pH on phytoplankton-bacterioplankton coupling at low nutrient conditions

The response of heterotrophic bacteria to changes in fCO_2 has been previously shown to be related to phytoplankton rather than being a direct effect of pH or CO_2 (e.g. Allgaier et al., 2008, Grossart et al., 2006a). Here, neither BPP nor BV of neither FL nor PA bacteria suggested a direct effect of CO_2 (PERMANOVA). Differences in FL bacterial BV, BPP and the ratio of HDNA/LDNA occurred along the gradient of fCO_2, but were limited to short time periods. Furthermore, these changes were not consistent with fCO_2 resulting in both increases and decreases of a particular variable at specific times (Fig. 1). Periods where fCO_2-related effects were apparent comprised periods with high organic matter turnover (e.g. breakdown of Chl *a* maximum). However, Paul et al. (2015) could not reveal any effect of fCO_2 on the export of carbon, neither across the study period nor at individual time points. Thus it is reasonable to assume that these small fCO_2-related differences in bacterial variables are a consequence of other altered components of the aquatic food web, and do not necessarily manifest as changes in carbon export.

Given the inability to relate individual aspects of microbial metabolism or community composition to fCO_2 concentrations, we sought to determine whether an impact was evident using a multivariate approach. Chemical, metabolic and community matrices exhibited large variations in relation to a strong temporal effect throughout the whole sampling period

(p<<0.01, Table 1, Table 3, Table 5). In addition, an effect of the fCO_2-treatment was also evident in all three multivariate assemblages, albeit explaining far less of the observed variability in chemical and metabolic variables (p<0.03, Table 1, Table 3, Table 5). However, when relating physiochemical to metabolic variables (DistLM, Table 4), neither fCO_2 nor pH were suitable to explaining the observed variability. In contrast, fCO_2 contributed to explaining the variability amongst the bacterioplankton-phytoplankton community dynamics (DistLM, Table 6). Taken together, this suggests that effects of fCO_2-treatments manifest indirectly, through either altering physiochemical parameters or more likely the composition of the microbial community with possible but so far hidden consequences for microbial metabolism.

4.3 fCO_2/pH effects on phytoplankton alter indirectly phytoplankton-bacterioplankton coupling at low nutrient conditions

Autotrophic organisms can be fertilized by an enhanced CO_2 availability, altering growth conditions of phytoplankton and increasing the production of particulate (POM) and dissolved organic matter (DOM) (Hein and Sand-Jensen, 1997; Riebesell et al., 2007). As a consequence of this increased photosynthetic fixation rate, both quantity and quality of dissolved organic matter (DOM) available for heterotrophic bacteria are impacted, with potential implications for the nature of coupling between phytoplankton and bacterioplankton at low nutrient conditions (Azam et al., 1983; Bratbak and Thingstad, 1985). So far, CO_2 enrichment experiments examining natural plankton assemblages (e.g. Engel, et al., 2005; Riebesell et al., 2007; Bach et al., 2016) did not reveal a consistent pattern of species response or primary production to elevated CO_2. Spilling et al. (2016a) could not detect any effect of increased CO_2 on total primary production, even though Crawfurd et al. (2016) reported effects of CO_2 on several groups of picophytoplankton. During our study, although one larger picoeukaryote (Pico III) was negatively impacted by fCO_2, two small picoeukaryotes (Pico I, Pico II) benefitted from the CO_2 addition, yielding significantly higher growth rates and BVs at higher fCO_2 (Crawfurd et al., 2016). This is consistent with recent evidence suggesting a positive impact of enhanced fCO_2 on the abundance of small picoeukaryotic phytoplankton (Brussaard et al., 2013; Newbold et al., 2012; Sala et al., 2015). Both picoeukaryotic groups were identified as variables explaining the separation along the fCO_2 gradient on the second and third dbRDA-axes in the DistLM ordination of the bacteria-phytoplankton community.

Specifically, Pico I was highly negatively correlated (r_s=-0.67) to dbRDA axis two. However, dbRDA indicated also opposing effects of fCO_2 on Pico II (r_s=0.54) and HDNA prokaryotes (r_s=-0.31), being positively or negatively correlated with axis three. Indeed, sharp increases in $BV_{Pico\ II}$ at high fCO_2 between t14-17 were associated with decreases in BV_{HDNA}.

Although we are not able to draw solid conclusions on the interaction of these two particular groups of organisms, a cluster analysis of pairwise Spearman correlations between functional groups of bacteria and phytoplankton revealed a distinct clustering with mesocosms based on fCO_2 concentration (Fig. 4). We also detected a change in the ratio of heterotrophic bacterial BV to Chl *a* between the different fCO_2-treatments, though this change was not visible for the entire study duration and not consistent with fCO_2. These results strongly suggest that trophic interactions between functional groups of bacteria and phytoplankton might be changing in a future acidified ocean.

In nutrient poor systems, variable growth rates of phytoplankton, DOM quality and quantity, but also losses of phyto- and bacterioplankton due to grazing or viral lyses may potentially contribute to this observed decoupling of phytoplankton and bacterioplankton at high fCO_2 (Azam et al., 1983; Bratbak and Thingstad, 1985; Sheik et al., 2014). The viral shunt or bacterivory may release phytoplankton from competition with bacteria for limiting nutrients (e.g. Bratbak and Thingstad, 1985; Caron and Goldman, 1990). How increased fCO_2 will affect these processes (e.g. viral lysis and bacterial grazing) under nutrient limited conditions remains so far uncertain. Bacterial grazing by mixotrophs, which would also directly benefit from increased CO_2 availability (Rose et al., 2009), may provide a mechanism for recycling of inorganic nutrients, otherwise bound in bacterial biomass, as a means for supporting phytoplankton growth (e.g. Mitra et al. 2014). However, other studies examining bacterial grazing under different nutrient conditions reported conflicting positive and negative results of increased fCO_2 (e.g. Brussaard et al., 2013; Rose et al., 2009). Although we are unable to draw defined conclusions on how this myriad of complex biological processes are impacted by fCO_2, it is very likely that there is an impact on trophic interactions which may account for the portion of unexplained variance we observed in our mulitvariate analyses.

5 Conclusion

The use of large-volume mesocosms allowed us to test for multiple fCO_2-related effects on dynamics of heterotrophic bacterial activity and their biovolume in a near-realistic ecosystem by including trophic interactions from microorganisms up to zooplankton. Complex interactions between various trophic levels, which can only be properly addressed at the scale of whole ecosystems, are important for understanding and predicting fCO_2-induced effects on aquatic food webs and biogeochemistry in a future, acidified ocean. We examined these impacts in a nutrient-depleted system, which is representative for large parts of the oceans (Moore et al., 2013). Heterotrophic bacterial productivity was, for the most part, tightly coupled to the availability of phytoplankton-derived organic matter. When accounting for temporal development and taking into account trophic interactions using multivariate statistics, changes in nutrient composition, metabolic parameters and bacteria-phytoplankton communities revealed a significant effect of the fCO_2-treatment. Although not consistent throughout the experiment, differences in the ratio of heterotrophic bacterial BV to Chl *a* during the last half of the experiment suggest that a future ocean will become more autotrophic during low productive periods as a result of altered trophic interactions between functional groups of bacteria and phytoplankton. There is additional support for this conclusion from examining the atmospheric exchange of CO_2 (Spilling et al., 2016b). During the limited time-scale of this study, the observed effects of fCO_2 did not manifest as altered carbon export (Paul et al., 2015). However, over several years, maintained changes in nutrient cycling, as a consequence of a permanent decoupling between bacteria and phytoplankton, are likely to arise and impact the nature of the carbon pump.

6 Data availability

Data of primary production and respiration can be obtained from Spilling et al. (2016b; doi: 10.1594/PANGAEA.863933). Other variables from the experiment (e.g. total particulate and dissolved nutrients) can be found in Paul et al. (2016; doi:10.1594/PANGAEA.863032). Flow cytometry data can be obtained from Crawfurd et al. (2016). A PANGEA data repository will be created for data of bacterial protein production and abundances of PA prokaryotes.

Acknowledgements

We thank the KOSMOS team and all of the participants in the mesocosm campaign for organisation, maintenance and support during the experiment. In particular, we would like to thank Andrea Ludwig for coordinating the campaign logistics and assistance with CTD operations, the diving team and Allanah Paul for her help in data acquisition. Further we thank the Tvärminne Zoological Station for the opportunity to carry out such a big mesocosm experiment at their research station and technical support on site. Additionally we acknowledge the captain and crew of R/V *ALKOR* for their work transporting, deploying (AL394) and recovering (AL397) the mesocosms. Further we thank the two reviewers for their critical comments to improve this manuscript. The collaborative mesocosm campaign was funded by BMBF projects BIOACID II (FKZ 03F06550) and SOPRAN Phase II (FKZ 03F0611). TH was further financially supported by DFG grant GR 1540/23-1 given to HPG. CPDB was financially supported by the Darwin project, the Royal Netherlands Institute for Sea Research (NIOZ), and the EU project MESOAQUA (grant agreement number 228224).

References

Agawin, N.S.R., Duarte, C.M., Agusti, S.: Nutrient and temperature control of the contribution of picoplankton to phytoplankton biomass and production, Limnol. Oceanogr., 45 (3), 591-600, 2000.

Allgaier, M., Riebesell, U., Vogt, M., Thyrhaug, R., Grossart, H.-P.: Coupling of heterotrophic bacteria to phytoplankton bloom development at different pCO_2 levels: a mesocosm study, Biogeosciences, 5, 1007-1022, 2008.

Anderson, M.J.: A new method for non-parametric multivariate analysis of variance, Austral. Ecol., 35, 32–46, 2001.

Anderson, M.J., Gorley, R.N. and Clarke, K.R.: PERMANOVA+ for PRIMER: Guide to Software and Statistical Methods, PRIMER-E, Plymouth, UK, 214, 2008.

Azam, F.: Microbial Control of Oceanic Carbon Flux: The Plot Thickens, Science, 280 (5364), 694-696, doi:10.1126/science.280.5364.694, 1998.

566 Azam, F., Fenchel, T., Field, J.G., Gray, J.S., Meyer-Reil, L.A., and Thingstad, F.: The
567 Ecological Role of Water-Column Microbes in the Sea, Mar. Ecol. Prog. Ser., 10, 257-263,
568 1983.

569 Bach, L.T., Taucher, J., Boxhammer, T., Ludwig, A., The Kristineberg KOSMOS
570 Consortium, Achterberg, E.P., Algueró-Muizñiz, M., Anderson, L.G., Bellworthy, J.,
571 Büdenbender, J., Czerny, J., Ericson, Y., Esposito, M., Fischer, M., Haunost, M., Hellemann,
572 D., Horn, H.G., Hornick, T., Meyer, J., Sswat, M., Zark, M., Riebesell, U.: Influence of Ocean
573 Acidification on a Natural Winter-to-Summer Plankton Succession: First Insights from a
574 Long-Term Mesocosm Study Draw Attention to Periods of Low Nutrient Concentrations.
575 PLoS ONE 11(8): e0159068, doi:10.1371/journal.pone.0159068, 2016.

576 Badr, E.-S. A., Achterberg, E. P., Tappin, A. D., Hill, S. J., and Braungardt, C. B.:
577 Determination of dissolved organic nitro-gen in natural waters using high-temperature
578 catalytic oxidation, TrAC-Trend, Anal. Chem., 22, 819–827, doi:10.1016/S0165-
579 9936(03)01202-0, 2003.

580 Benjamini, Y., and Hochberg, Y.: Controlling the false discovery rate: a practival and
581 powerful approach to multiple testing. Journal of the Royal Statistical Society Series B, 57,
582 289-300, 1995.

583 Berggren, M., Lapierre, J.-F., and del Giorgio, P. A.: Magnitude and regulation of
584 bacterioplankton respiratory quotient across fresh-water environmental gradients, ISME
585 Journal, 6, 984–993, 2012.

586 Bratbak, G., Thingstad, T.F.: Phytoplankton-bacteria interactions: an apparent paradox?
587 Analysis of a model system with both competition and commensalism. Mar. Ecol. Prog. Ser.,
588 25, 23-30, 1985.

589 Brussaard, C.P.C., Noordeloos, A.A.M., Witte, H., Collenteur, M.C.J., Schulz, K.G., Ludwig,
590 A., Riebesell, U.: Arctic microbial community dynamics influenced by elevated CO_2 levels,
591 Biogeosciences, 10, 719-731, 2013.

592 Caldeira, K. and Wickett, M.E.: Anthropogenic carbon and ocean pH, Nature, 425, 365, 2003.

593 Caron, D.A., Goldman, J.C.: Protozoan nutrient regeneration. In: Capriulo GM (Ed.) Ecology
594 of marine protozoa, Oxford University Press, New York, p 283–306, 1990.

595 Clarke, K.R. and Gorley, R.N.: PRIMER v6: User manual/tutorial, PRIMER-E, Plymouth,
596 UK, 115 pp., 2006.

597 Crawfurd, K.J., Riebesell, U., and Brussaard, C.P.D.: Shifts in the microbial community in the
598 Baltic Sea with increasing CO_2, Biogeosciences Discuss., doi:10.5194/bg-2015-606, in
599 review, 2016.

600 Dickson, A.G., Sabine, C., and Christian, J. (Eds.): Guide to best practices for ocean CO_2
601 measurements, PICES Special Publication 3, 191 pp., http://aquaticcommons.org/1443/ (last
602 access: 16 October 2012), 2007.

603 Drakare, S., Blomqvist, P., Bergström, A.-K. and Jansson, M.: Relationships between
604 picophytoplankton and environmental variables in lakes along a gradient of water colour and
605 nutrient content, Freshwater Biology, 48, 729-740, 2003.

606 Engel, A., Zondervan, I., Aerts, K., Beaufort, L., Benthien, A., Chou, L., Delille, B., Gattuso,
607 J.-P., Harlay, J., and Heemann, C.: Testing the direct effect of CO_2 concentration on a bloom
608 of the coccolithophorid Emiliania huxleyi in mesocosm experiments, Limnol. Oceanogr., 50,
609 493–507, doi:10.4319/lo.2005.50.2.0493, 2005.

610 Gargas, E.: A manual for phytoplankton primary production studies in the Baltic, The Baltic
611 Marine Biologist, Hørsholm, Denmark, 88 pp., 1975.

612 Grasshoff, K., Ehrhardt, M., Kremling, K., and Almgren, T.: Methods of seawater analysis,
613 Wiley Verlag Chemie GmbH, Weinheim, Germany, 1983.

614 Grossart, H.-P.: Ecological consequences of bacterioplankton lifestyles: changes in concepts
615 are needed. Environ. Microbiol. Rep., 2, 706–714. doi: 10.1111/j.1758-2229.2010.00179.x,
616 2010.

617 Grossart, H.-P. and Simon, M.: Limnetic macroscopic organic aggregates (lake snow):
618 Occurrence, characteristics, and microsbial dynamics in Lake Constance, Limnol. Oceanogr.,
619 38, 532-546, 1993.

620 Grossart, H.-P., Allgaier, M., Passow, U., Riebesell, U.: Testing the effect of CO_2
621 concentration on the dynamics of marine heterotrophic bacterioplankton, Limnology and
622 Oceanography, 51, 1-11, 2006a

623 Grossart, H.-P., Czub, G., and Simon, M.: Specific interactions of planktonic algae and
624 bacteria: Implications for aggregation and organic matter cycling in the sea, Environ.
625 Microbiol., 8, 1074–1084, 2006b.

626 Hagström, Å., Larsson, U., Hörstedt, P., Normark, S.: Frequency of Dividing Cells, a New
627 Approach to the Determination of Bacterial Growth Rates in Aquatic Environments, Appl.
628 Environ. Microbiol., 37 (5), 805-812, 1979.

629 Hansen, H. P. and Koroleff, F.: Determination of nutrients, in Methods of Seawater Analysis,
630 edited by: Grasshoff, K., Kremling, K., and Ehrhardt, M., Wiley Verlag Chemie GmbH,
631 Zeinheim, Germany, 159–228, 1999.

632 Harrell, F.E. Jr., with contributions from Dupont, C. and many others: Hmisc: Harrell
633 Miscellaneous. R package version 3.17-4, httpx:// CRAN.R-project.org/package=Hmisc,
634 2016.

635 Hein, M. and Sand-Jensen, K.: CO_2 increases oceanic primary production, Nature, 388, 526-
636 527, doi:10.1038/41457, 1997.

637 Hobbie, J.E., Daley, R.J., Jasper, S.: Use of nuclepore filters for counting bacteria by
638 fluorescence microscopy, Appl. Environ. Microbiol., 33, 1225-1228, 1977.

639 Hoikkala, L., Aarnos, H., Lignell, R.: Changes in Nutrient and Carbon Availability and
640 Temperature as Factors Controlling Bacterial Growth in the Northern Baltic Sea., Estuaries
641 and Coasts, 32, 720-733, doi:10.1007/s12237-009-9154-z, 2009.

642 Joint, I., Henriksen, P., Fonnes, G.A., Bourne, D., Thingstad, T.F., Riemann, B.: Competition
643 for inorganic nutrients between phytoplankton and bacterioplankton in nutrient manipulated
644 mesocosms, Aqut. Microb. Ecol., 29, 145-159, 2002.

645 Kirchman, D.L.: The Uptake of Inorganic Nutrients by Heterotrophic Bacteria, Microb. Ecol.,
646 28, 255-271, 1994

647 Kirchman, D.L., Elifantz, H., Dittel, A.I., Malmstrom, R.R. and Cottrell, M.T.: Standing
648 stocks and activity of Archaea and Bacteria in the western Arctic Ocean, Limnol. Oceanogr.,
649 52 (2), 495-507, 2007.

650 Kuparinen, J. and Heinänen, A.: Inorganic Nutrient and Carbon Controlled Bacterioplankton
651 Growth in the Baltic Sea. Estuarine, Coastal and Shelf Science 37: 271–285, 1993.

652 Lapoussière, A., Michel, C., Starr, M., Gosselin, M., Poulin, M.: Role of free-living and
653 particle-attached bacteria in the recycling and export of organic material in the Hudson Bay
654 system, Journal of Marine Systems, 88, 434-445, 2011.

655 Legendre, P. and Anderson, M.J.: Distance-based redundancy analysis: testing multispecies
656 responses in multifactorial ecological experiments. Ecol. Monogr., 69, 1–24, 1999.

657 Lignell, R., Hoikkala, L., Lahtinen, T.: Effects of inorganic nutrients, glucose and solar
658 radiation treatments on bacterial growth and exploitation of dissolved organic carbon and
659 nitrogen in the northern Baltic Sea. Aquat. Microb. Ecol., 51, 209–221, 2008.

660 Lueker, T.J., Dickson, A.G., and Keeling, C.D.: Ocean pCO2 calculated from dissolved
661 inorganic carbon, alkalinity, and equations for K1 and K2: validation based on laboratory
662 measurements of CO2 in gas and seawater at equilibrium, Mar. Chem., 70, 105-119,
663 doi:10.1016/S0304-4203(00)00022-0, 2000.

664 Maat, D.S., Crawfurd, K.J., Timmermans, K.R. and Brussaard, C.P.D.: Elevated CO_2 and
665 Phosphate Limitation Favor *Micromonas pusilla* through Stimulated Growth and Reduced
666 Viral Impact, Appl. Environ. Microbiol., 80 (10), 3119-3127, doi:10.1128/AEM.03639-13,
667 2014.

668 Marie, D., Brussaard, C.P.D., Thyrhaug, R., Bratbak, G., Vaulot, D.: Enumeration of marine
669 viruses in culture and natural samples by flow cytometry, Appl. Environ. Microbiol., 65(1),
670 45-52, 1999.

671 Massana, R., Gasol, J.M., Bjørnsen, P.K., Blackburn, N., Hagström, Å, Hietanen, S., Hygum,
672 B.H., Kuparinen and Pedrós-Alió C.: Measurement of bacterial size via image analysis of
673 epifluorescence preparations: description of an inexpensive system and solutions to some of
674 the most common problems, Sci. Mar., 61(3), 397-407, 1997.

675 Mehrbach, C., Culberson, C.H., Hawley, J.E., and Pytkowicz, R.M.: Measurement of apparent
676 dissociation constants of carbonic acid in seawater at atmospheric pressure, Limnol.
677 Oceanogr., 18, 897-807, 1973.

678 Mitra, A., Flynn, K.J., Burkholder, J.M., Berge, T., Calbet, A., Raven, J.A., Granéli, E.,
679 Gilbert, P.M., Hansen, P.J., Stoecker, D.K., Thingstad, F., Tillmann, U., Våge, S., Wilken, S.,
680 and Zubkov, M.V.: The role of mixotrophic protists in the biological carbon pump,
681 Biogeosciences, 11, 995-1005, doi:10.5194/bg-11-995-2014, 2014.

682 Moore, C.M., Mills, M.M., Arrigo, K.R., Berman-Frank, I, Bopp, L., Boyd, P.W., Galbraith,
683 E.D., Geider, R.J., Guieu, C., Jaccard, S.L., Jickells, T.D., La Roche, J., Lenton, T.M.,
684 Mahowald, N.M., Marañón, E., Marinov, I., Moore, J.K., Nakatsuka, T., Oschlies, A., Sito,
685 M.A., Thingstad, T.F., Tsuda, A. and Ulloa, O.: Processes and patterns of oceanic nutrient
686 limitation, Nature Geoscience, 6(9), 701-710, doi:10.1038/NGEO1765, 2013.

687 Nausch, M., Bach, L.T., Czerny, J., Godstein, J., Grossart, H.-P., Hellemann, D., Hornick, T.,
688 Achterberg, E.P., Schulz, K.-G., and Riebesell, U.: Effects of CO_2 perturbation on phosphorus
689 pool sizes and uptake in a mesocosm experiment during a low productive summer season in
690 the northern Baltic Sea, Biogeosciences, 13, 3035-3050, doi:10.5194/bg-13-3035-2016, 2016.

691 Newbold, L., Oliver, A.E., Booth, T., Tiwari, B., DeSantis, T., Maguire, M., Andersen, G.,
692 van der Gast, C.J., and Whiteley, A.S.: The response of marine picoplankton to ocean
693 acidification, Environmental Microbiology, 14 (9), 2293-2307, 2012.

694 Oksanen, J., Blanchet, F.G., Friendly, M., Kindt, R., Legendre, P., McGlinn, D., Minchin,
695 P.R., O`Hara, R.B., Simpson, G.L., Solymos, P., Stevens, M.H.H., Szoecs, E., and Wagner,
696 H.: vegan: Community Ecology Package. R package version 2.4-0, https://CRAN.R-
697 project.org/package=vegan, 2016.

698 Patey, M. D., Rijkenberg, M. J. A., Statham, P. J., Stinchcombe, M. C., Achterberg, E. P., and
699 Mowlem, M.: Determination of nitrate and phosphate in seawater at nanomolar
700 concentrations, TrAC-Trend, Anal. Chem., 27, 169–182, doi:10.1016/j.trac.2007.12.006,
701 2008.

702 Paul, A.J., Bach, L.T., Schulz, K.-G., Boxhammer, T., Czerny, J., Achterberg, E.P.,
703 Hellemann, D., Trense, Y., Nausch, M., Sswat, M., Riebesell, U.: Effect of elevated CO_2 on
704 orgnaic matter pools and fluxes in a summer Baltic Sea plankton community, Biogeosciences,
705 12, 1-23, doi:10.5194/bg-12-1-2015, 2015.

706 Porter, K.G., Feig, Y.S.: Dapi for identifying and counting aquatic microflora, Limnol.
707 Oceanogr., 25, 943-948, 1980.

708 Raven, J.A.: The twelfth Tansley Lecture. Small is beautiful: the picophytoplankton,
709 Functional Ecology, 12, 503-513, 1998.

710 R Core Team (2016). R: A language and environment for statistical computing. R Foundation
711 for Statistical Computing, Vienna, Austria, URL http://www.R-project.org/, 2014.

712 Riebesell, U., Gattuso, J.-P.: Lessons learned from ocean acidification research. Reflection on
713 the rapidly growing field of ocean acidification research highlights priorities for future
714 research on the changing ocean. Nature Climate Change, 5, 12-14, doi:10.1038/nclimate2456,
715 2015.

716 Riebesell, U., Schulz, K.G., Bellerby, R.G.J., Botros, M., Fritsche, P., Meyerhöfer, M., Neill,
717 C., Nondal, G., Oschlies, A., Wohlers and J., Zöllner, E.: Enhanced biological carbon
718 consumption in a high CO_2 ocean, Nature Letters, 450 (22), 545-548,
719 doi:10.1038/nature06267, 2007.

720 Rieck, A., Herlemann, D.P.R., Jürgens, K. and Grossart, H.-P.: Particle-Associated Differ
721 from Free-Living Bacteria in Surface Waters of the Baltic Sea, Front. Microbiol., 6 (1297),
722 doi:10.3389/fmicb.2015.01297, 2015.

723 Rose, J.M., Feng, Y., Gobler, C.J., Gutierrez, R., Hare, C.E., Leblanc, K., Hutchins, D.A.:
724 Effects of increased pCO2 and temperature on the North Atlantic spring bloom. II.
725 Microzooplankton abundance and grazing, Mar. Ecol. Prog. Ser., 388, 27-40, 2009.

726 Sala, M.M., Aparicio, F.L., Balagué, V., Boras, A., Borrull, E., Cardelús, C., Cros, L., Gomes,
727 A., López-Sanz, A., Malits, A., Martinez, R.A., Mestre, M., Movilla, J., Sarmento, H.,
728 Vázquez-Dominguez, E., Vaqué, D., Pinhassi, J., Calbet, A., Calvo, E., Gasol, J.M., Pelejero,
729 C., Marrasé, C.: Contrasting effects of ocean acidification on the microbial food web under
730 different trophic conditions, ICES Journal of Marine Science, doi:10.1093/icesjms/fsv130,
731 2015.

732 Sharp, J.: Improved analysis for particulate organic carbon and nitrogen from seawater,
733 Limnol. Oceanogr., 19, 984–989, 1974.

734 Sheik, A.R., Brussaard, C.P.D., Lavik, G., Lam, P., Musat, N., Krupke, A., Littmann, S.,
735 Strous, M. and Kuypers M.M.M.: Responses of the coastal bacterial community to viral
736 infection of the algae Phaeocystic globosa, The ISME Jounal, 8, 212-225, doi:
737 10.1038/ismej.2013.135, 2014.

738 Simon, M., Azam, F.: Protein content and protein synthesis rates of planktonic marine
739 bacteria, Marine Ecology Progress Series, 51, 201-213, 1989.

740 Smith, D.C., Simon, M., Alldredge, A.L., Azam, F.: Intense hydrolytic enzyme activity on
741 marine aggregates and implications for rapid particle dissolution, Nature, 359, 139-142, 1992.

742 Spilling, K., Paul, A.J., Virkkala, N., Hastings, T., Lischka, S., Stuhr, A., Bermudéz, R.,
743 Czerny, J., Boxhammer, T., Schulz, K.G., Ludwig, A., and Riebesell, U.: Ocean acidification
744 decreases plankton respiration: evidence from a mesocosm experiment, Biogeosciences, 13,
745 4707-4719, doi:10.5194/bg-13-4707-2016, 2016a.

746 Spilling, K., Schulz, K. G., Paul, A. J., Boxhammer, T., Achterberg, E. P., Hornick, T.,
747 Lischka, S., Stuhr, A., Bermúdez, R., Czerny, J., Crawfurd, K.J., Brussaard, C. P. D.,
748 Grossart, H.-P., and Riebesell, U.: Effects of ocean acidification on pelagic carbon fluxes in a
749 mesocosm experiment, Biogeosciences Discuss., doi:10.5194/bg-2016-56, in review, 2016b.

750 Steeman-Nielsen, E.: The use of radioactive carbon for measuring organic production in the
751 sea, J. Cons. Int. Explor. Mer., 18, 117–140, 1952.

752 Suttle, C.A., Fuhrman, J.A., Capone, D.G.: Rapid ammonium cycling and concentration-
753 dependent partitioning of ammonium and phosphate: Implications for carbon transfer in
754 planktonic communities, Limnol. Oceanogr., 35 (2), 424-433, 1990.

755 Suzuki, R., Shimodaira, H.: pvclust: Hierarchical Clustering with p-values via Multiscale
756 Bootstrap Resampling, R package version 2.0-0., https://CRAN.R-
757 project.org/package=pvclust, 2015.

758 Taylor, A.R., Brownlee, C., Wheeler, G.L.: Proton channels in algae: reasons to be excited,
759 Trends in Plant Sciences, 17(11), 675-684, doi:10.1016/ j.tplants.2012.06.009, 2012

760 Thingstad, T.F., Hagström, Å., Rassoulzadegan, F.: Accumulation of degradable DOC in
761 surface waters: Is it caused by a malfunctioning microbial loop?, Limnol. Oceanogr., 42(2),
762 398-404, 1997.

763 Thingstad, T.F., Bellerby, R.G.J., Bratbak, G., Borsheim, K.Y., Egge, J.K., Heldal, M.,
764 Larsen, A., Neill, C., Nejstgaard, J., Norland, S., Sandaa, R.-A., Skjoldal, E.F., Tanaka, T.,
765 Thyrhaug, R., Töpper, B.: Counterintuitive carbon-to-nutrient coupling in an Arctic pelagic
766 ecosystem, Nature Letters, 455, 387-391, doi:10.1038/nature07235, 2008.

767 Toggweiler, J.R.: Carbon overconsumption, Nature, 363, 210-211, 1993.

768 Warnes, G.R., Bolker, B., Bonebakker, L., Gentleman, R., Liaw, W.H.A., Lumley, T.,
769 Maechler, M., Magnusson, A., Moeller, S., Schwartz, M., and Venables, B.: gplots: Various R

Programming Tools for Plotting Data. R package version 3.0.1, https://CRAN.R-project.org/package=gplots, 2016.

Welschmeyer, N. A.: Fluorometric analysis of chlorophyll a in the presence of chlorophyll b and pheopigments, Limnol. Oceanogr., 39, 1985–1992, doi:10.4319/lo.1994.39.8.1985, 1994.

Wickham, H.: ggplot2: Elegant graphics for data analysis. Springer-Verlag New York, 2009.

Table 1: Results of two-factor permutational multivariate analysis of variance (PERMANOVA)[(*)] on a resemblance matrix (Euclidian distance) of normalized chemical varables (Phosphate, DOC, TDN, DSi, TPC, PON, POP, BSi). Time (Ti); fCO_2-treatment (fCO_2); Residuals (Res).

Source of variation	*df*	SS	MS	Pseudo-*F*	*p (perm)*	Unique perms
Time	9	309.93	34.436	11.118	**0.0001**	9920
fCO_2 [(**)]	4	31.974	7.9936	2.5808	**0.0246**	9936
Time x fCO_2	36	80.177	2.2271	0.71906	0.8794	9904
Res	10	30.973	3.0973			
Total	59	472				

[(*)] Permutation was performed with unrestricted permutation of raw data.

[(**)] Pair-wise test could only be performed for control-mesocosms (n=2) with each fCO_2-treatment (n=1), due to missing replication for each fCO_2-treatment. Pair-wise comparison was only significant between control and the highest fCO_2-treatment (p_{perm}=0.029).

Table 2: Eigenvectors and -values of the first four axes of a PCA on normalized variables of dissolved and particulate nutrients. Ordination of the PCA is visualized in Fig. 6.

Variable	PC1	PC2	PC3	PC4
DOC	-0.4	-0.23	0.04	0.68
TDN	0.39	0.21	0.21	0.47
Phosphate	-0.1	0.48	-0.74	0.35
DSi	0.3	0.52	-0.03	-0.24
TPC	0.48	-0.06	0.03	0.13
PON	0.46	-0.05	-0.05	0.16
POP	0.36	-0.39	-0.04	0.21
BSi	0.17	-0.51	-0.63	-0.22
% variation	49.2	19.7	11.4	7.2
cum. % variation	49.2	68.9	80.4	87.6

Table 3: Results of two-factor permutational multivariate analysis of variance (PERMANOVA)[(*)] on a resemblance matrix (Euclidian distance) based on normalized metabolic variables (bacterial protein production (BPP), areal primary production (PP) and community respiration (CR)). Time (Ti); fCO_2-treatment (fCO_2); Residuals (Res).

Source of variation	***df***	**SS**	**MS**	**Pseudo-*F***	***p (perm)***	**Unique perms**
Time	9	92.128	10.236	6.73	**0.001**	9931
fCO_2 [(**)]	4	16.044	4.011	2.637	**0.023**	9944
Time x fCO_2	36	42.721	1.1867	0.78018	0.792	9904
Res	10	15.21	1.521			
Total	59	182.46				

[(*)] Permutation was performed with unrestricted permutation of raw data.

[(**)] Pair-wise test could only be performed for control-mesocosms (n=2) with each fCO_2-treatment (n=1), due to missing replication for each fCO_2-treatment. Pair-wise comparisons were significant between control and all fCO_2-treatments ($p_{perm}<0.04$).

Table 4: Summary of a DistLM procedure for modelling the relationship between physicochemical variables and a resemblance matrix based on a multivariate assemblage comprising normalized data of bacterial protein production (BPP), areal primary production (PP) and community respiration (CR). Non-redundant physicochemical variables were removed prior analysis. Therefore PON and pH were excluded from the subsequent analysis due to high correlations (r_s>0.9) to TPC and fCO_2, respectively.

Variable	SS (trace)	Pseudo-*F*	*p*	Prop.
fCO_2	5.0551	1.6527	0.1759	0.03
Temp$^{(*)}$	10.209	3.4376	**0.0229**	0.055
PAR$^{(*)}$	6.2466	2.056	0.1067	0.034
DOC$^{(*)}$	8.6228	2.8769	**0.0474**	0.047
TDN	4.7628	1.5545	0.1984	0.026
Phosphate$^{(*)}$	12.319	4.1994	**0.0111**	0.068
DSi	0.26167	0.083	0.9648	0.001
TPC	7.7827	2.5842	0.0613	0.004
POP	5.0171	1.6399	0.1818	0.027
BSi	11.688	3.9696	**0.0111**	0.064

$^{(*)}$ variables selected in step-wise procedure based on AIC.

Table 5: Results of two-factor permutational multivariate analysis of variance (PERMANOVA)[*] on a resemblance matrix (Bray Curtis similarity) based on log(X+1) transformed abundances of Pico I-III, Nano I-II, FL bacteria (HDNA, LDNA), PA bacteria, Cyanobacteria and Chl *a*. Time (Ti); fCO_2-treatment (fCO_2); Residuals (Res).

Source of variation	*df*	SS	MS	Pseudo-*F*	*p (perm)*	Unique perms
Time	9	201.83	22.426	56.754	**0.0001**	9923
fCO_2 [**]	4	23.631	5.9077	14.951	**0.0001**	9940
Time x fCO_2	36	19.859	0.55164	1.396	0.151	9915
Res	10	3.9515	0.39515			
Total	59	271.01				

[*] Permutation was performed with unrestricted permutation of raw data.

[**] Pair-wise test could only be performed for control-mesocosms (n=2) with each fCO_2-treatment (n=1), due to missing replication for each fCO_2-treatment. Pair-wise comparisons were significant between control and all fCO_2-treatments ($p_{perm}<0.01$).

Table 6: Summary of a DistLM procedure for modelling the relationship between physicochemical variables and a multivariate assemblage comprising variables of the bacterial and phytoplankton community. The resemblance matrix (Bray Curtis similarity) was based on log(X+1) transformed abundances of Pico I-III, Nano I-II, FL bacteria (HDNA, LDNA), PA bacteria, *Synechococcus* spp. and Chl *a*. Non-redundant physicochemical variables were removed prior analysis. Therefore PON and pH were excluded from the subsequent analysis due to high correlations (r_s>0.9) to TPC and fCO_2, respectively.

Variable	SS (trace)	Pseudo-*F*	*p*	Prop.
fCO_2 $^{(*)}$	20.469	4.7386	**0.0119**	0.075
Temp$^{(*)}$	51.838	13.718	**0.0001**	0.191
PAR	10.791	2.4051	0.0813	0.039
DOC	11.14	2.4864	**0.0769**	0.041
TDN	9.4456	2.0945	0.1078	0.034
Phosphate$^{(*)}$	25.649	6.063	**0.0029**	0.095
DSi	9.5766	2.1246	0.103	0.035
TPC$^{(*)}$	36.038	8.8955	**0.0002**	0.133
POP	52.171	13.827	**0.0001**	0.193
BSi	36.439	9.01	**0.0005**	0.134

$^{(*)}$ variables selected in step-wise procedure based on AIC.

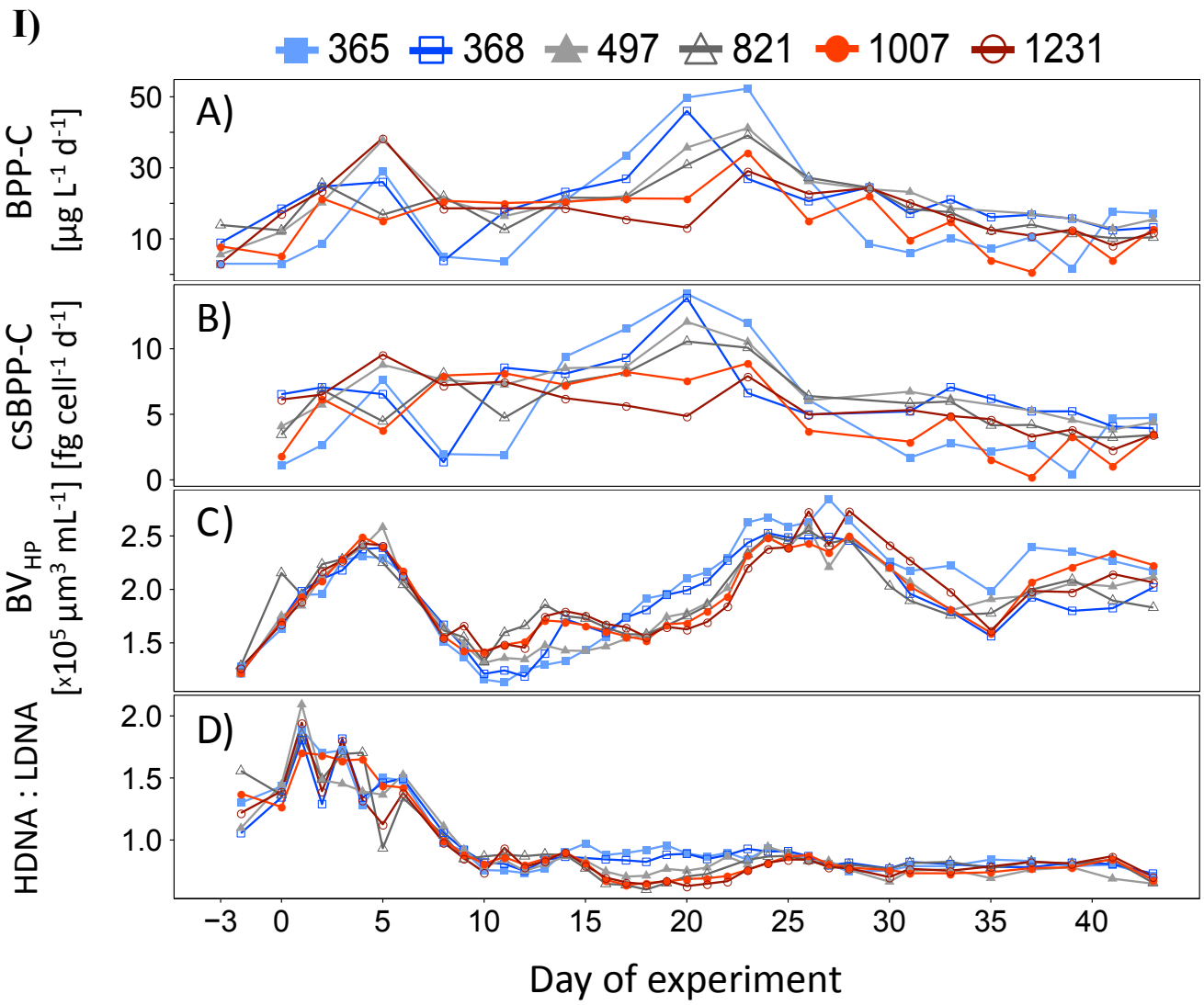
I)
365
368
497
821
1007
1231
A)
B)
C)
D)
BPP-C [µg L-1 d-1]
csBPP-C [fg cell-1 d-1]
BVHP [×10^5 µm^3 mL-1]
HDNA : LDNA
Day of experiment

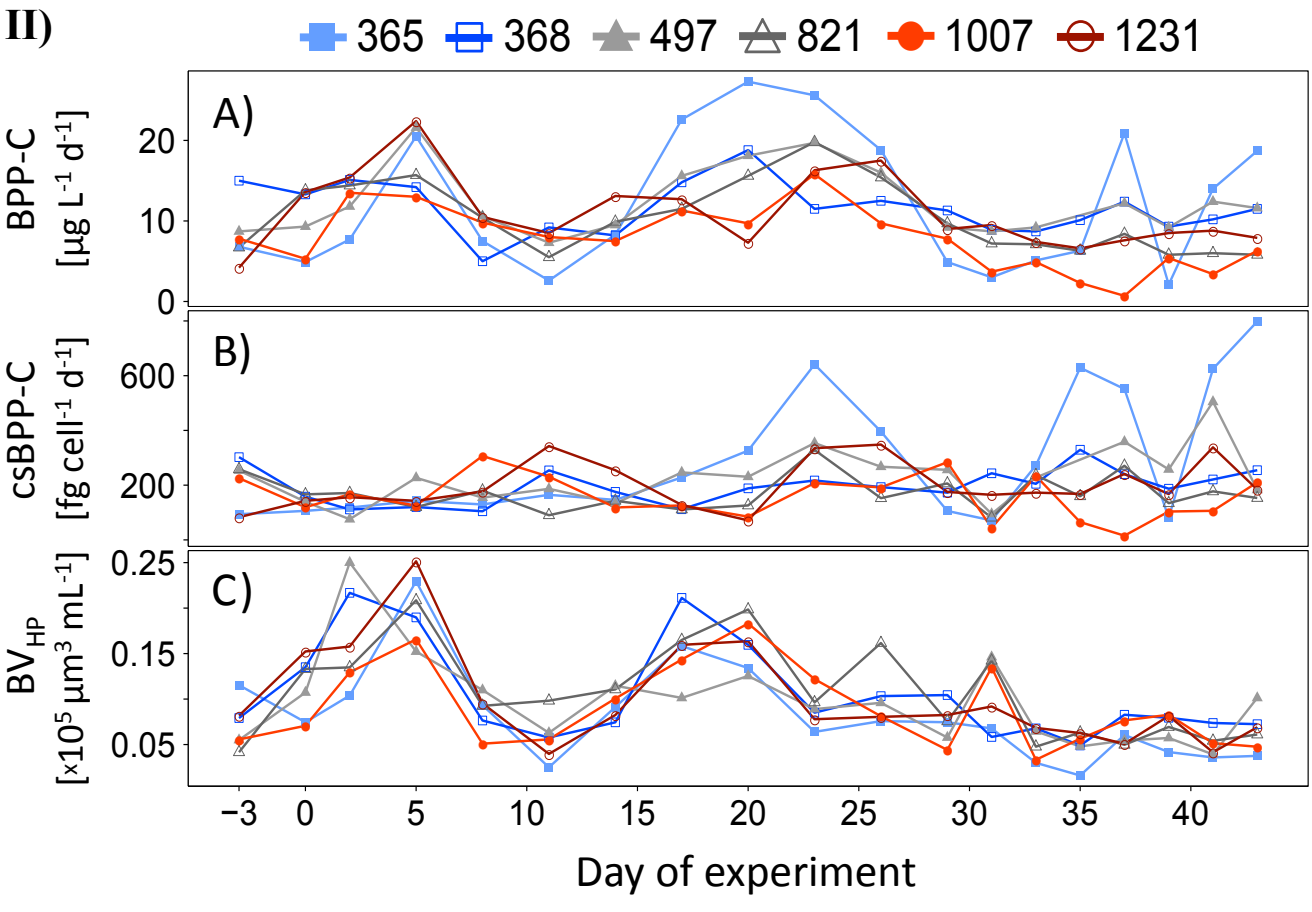
II)
365
368
497
821
1007
1231
A)
B)
C)
BPP-C [µg L-1 d-1]
csBPP-C [fg cell-1 d-1]
BVHP [×10^5 µm^3 mL-1]
Day of experiment

Figure 1. A) Bacterial Protein Production (BPP-C) [$\mu g\ L^{-1}\ d^{-1}$], B) cell-specific Bacterial Protein Production (csBPP-C) [$fg\ cell^{-1}\ d^{-1}$] and C) biovolume of heterotrophic prokaryotes (BV_{HP}) [$x10^5\ \mu m^3\ ml^{-1}$] of size fractions I) 0.2-5.0 µm (free-living bacteria) and II) >5.0 µm (particle-associated bacteria) during the course of the experiment. I-D) Ratio of high versus low nucleic acid stained prokaryotic heterotrophs (HDNA:LDNA), which both made up free-living BV_{HP}, revealed from flow cytometry. Colours and symbols indicate average fCO_2 [µatm] between t1-t43.

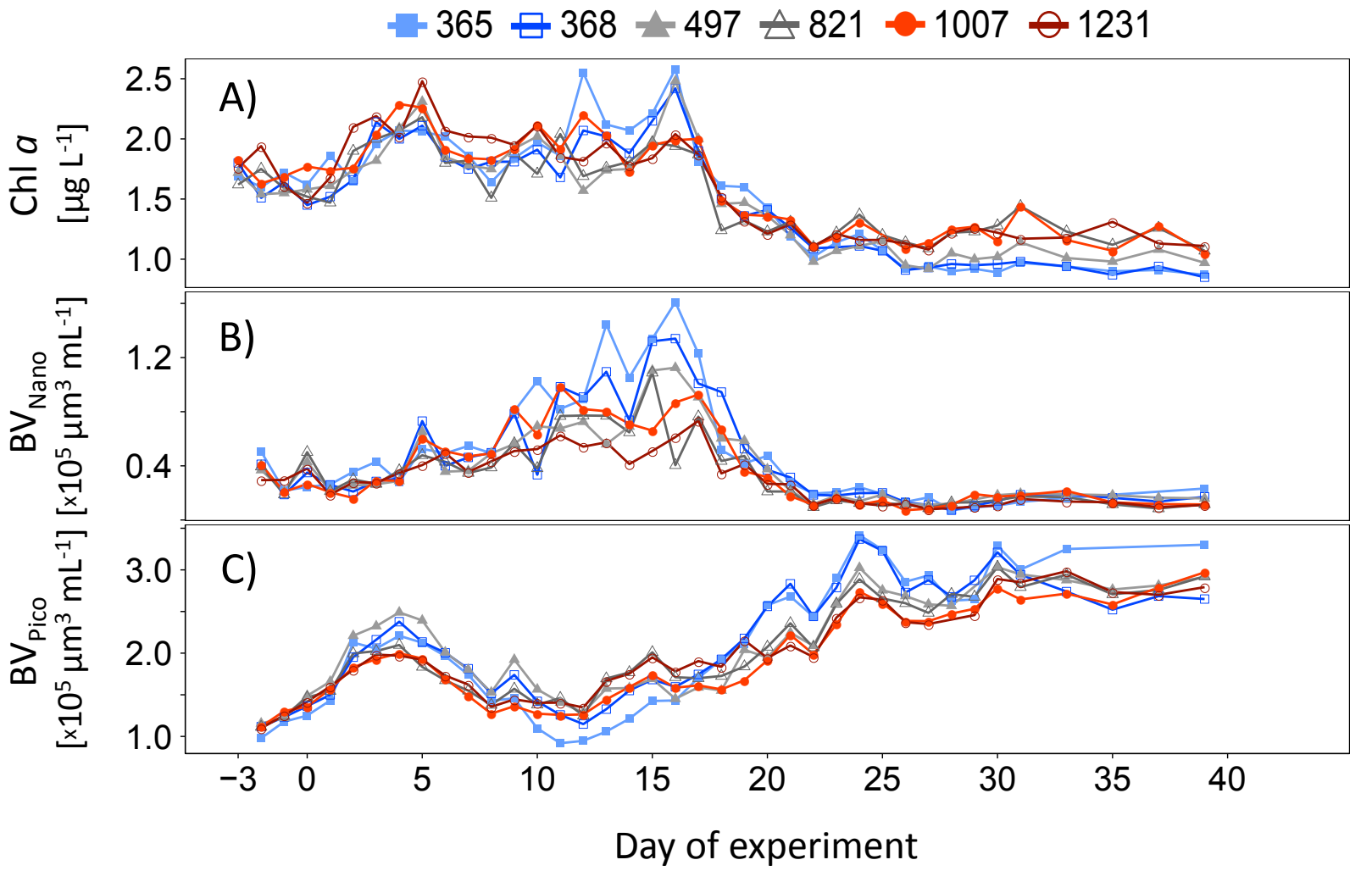
365
368
497
821
1007
1231
A)
B)
C)
Chl a [µg L-1]
BVNano [x105 µm3 mL-1]
BVPico [x105 µm3 mL-1]
2.5
2.0
1.5
1.0
1.2
0.4
3.0
2.0
1.0
−3
0
5
10
15
20
25
30
35
40
Day of experiment

Figure 2. A) Concentration of chlorophyll *a* [µg L^{-1}], B) biovolume of nanophytoplankton (Nano I and Nano II) [x10^5 µm^3 ml^{-1}] and C) biovolume of picophytoplankton (*Synechococcus* spp., Pico I-III) [x10^5 µm^3 ml^{-1}] during the course of the experiment. Colours and symbols indicate average fCO_2 [µatm] between t1-t43.

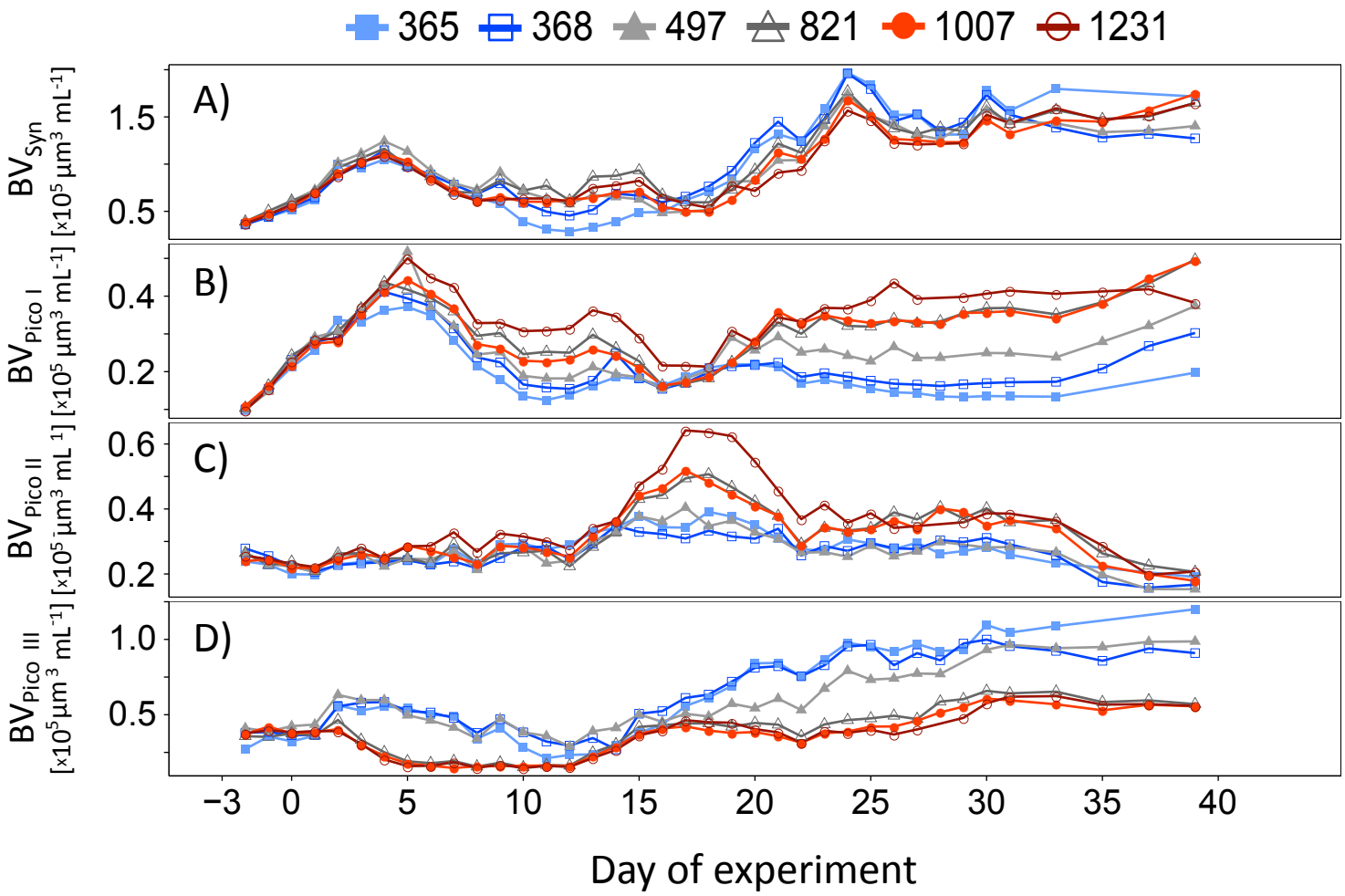
365
368
497
821
1007
1231
A)
B)
C)
D)
BV Syn [x10^5 µm^3 mL^-1]
BV Pico I [x10^5 µm^3 mL^-1]
BV Pico II [x10^5 µm^3 mL^-1]
BV Pico III [x10^5 µm^3 mL^-1]
1.5
0.5
0.4
0.2
0.6
0.4
0.2
1.0
0.5
−3
0
5
10
15
20
25
30
35
40
Day of experiment

Figure 3. A) Biovolume of *Synechococcus* spp. [$x10^5\ \mu m^3\ ml^{-1}$] and B-D) biovolume of picoeukaryote groups I-III (Pico I-III) [$x10^5\ \mu m^3\ ml^{-1}$] during the course of the experiment. Colours and symbols indicate average fCO_2 [µatm] between t1-t43.

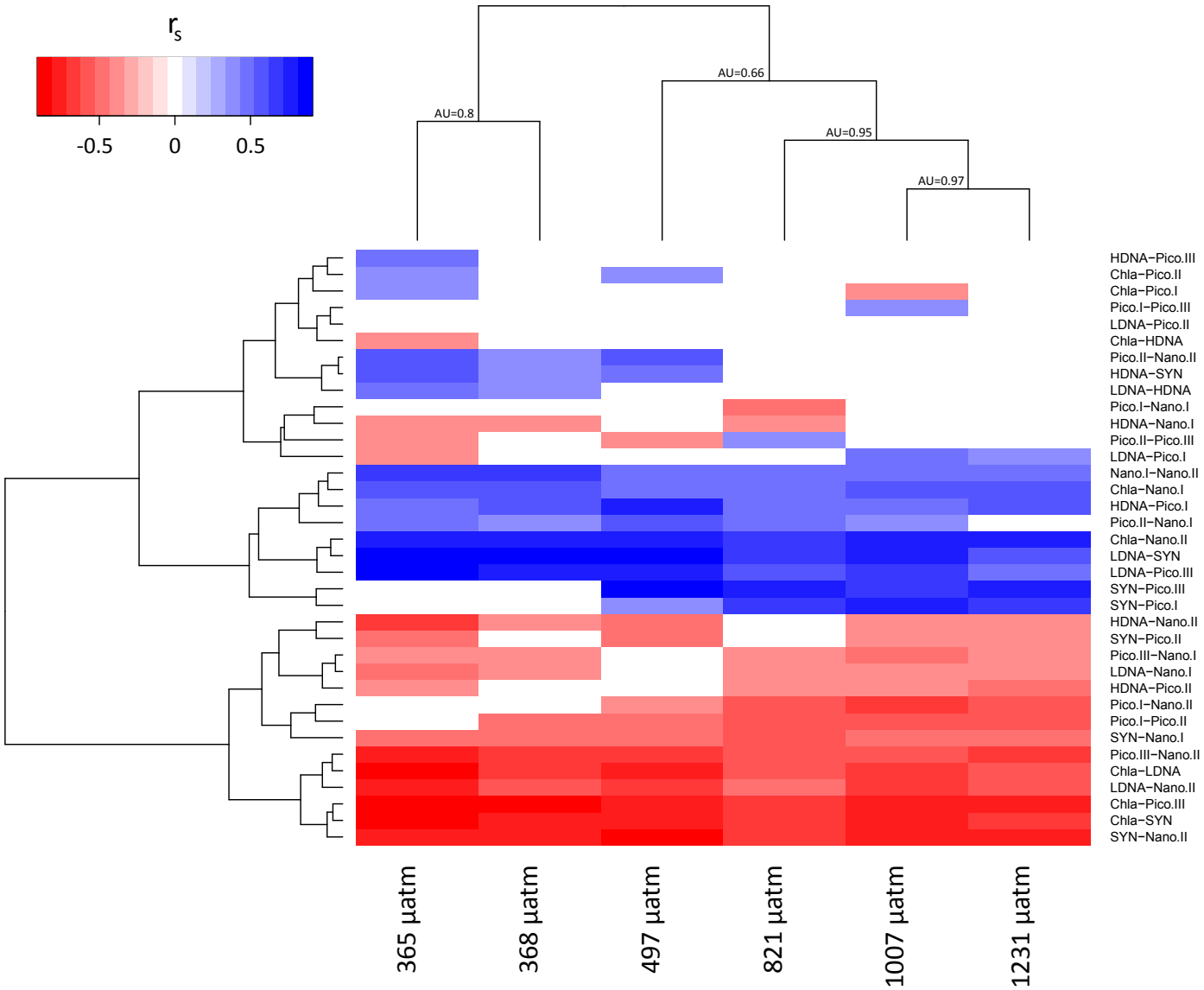
r_s
-0.5
0
0.5
AU=0.8
AU=0.66
AU=0.95
AU=0.97
HDNA−Pico.III
Chla−Pico.II
Chla−Pico.I
Pico.I−Pico.III
LDNA−Pico.II
Chla−HDNA
Pico.II−Nano.II
HDNA−SYN
LDNA−HDNA
Pico.I−Nano.I
HDNA−Nano.I
Pico.II−Pico.III
LDNA−Pico.I
Nano.I−Nano.II
Chla−Nano.I
HDNA−Pico.I
Pico.II−Nano.I
Chla−Nano.II
LDNA−SYN
LDNA−Pico.III
SYN−Pico.III
SYN−Pico.I
HDNA−Nano.II
SYN−Pico.II
Pico.III−Nano.I
LDNA−Nano.I
HDNA−Pico.II
Pico.I−Nano.II
Pico.I−Pico.II
SYN−Nano.I
Pico.III−Nano.II
Chla−LDNA
LDNA−Nano.II
Chla−Pico.III
Chla−SYN
SYN−Nano.II
365 µatm
368 µatm
497 µatm
821 µatm
1007 µatm
1231 µatm

Figure 4. Heatmap and cluster analysis based on significant Spearman`s rank correlation coefficients calculated for each mesocosm between all possible combinations of abundances between different functional heterotrophic prokaryotic and phytoplanktonic groups (high and low nucleic acid stained prokaryotic heterotrophs (HDNA; LDNA), *Synechococcus* spp. (SYN), picoeukaryotes I-III (Pico I-III), nanophytoplankton I-II (Nano I-II)) and Chl *a* based on daily measurements between t1 and t39. Colours indicate the Spearman`r rank coefficient (r_s) between two variables. *P*-values of correlations were corrected for multiple testing according Benjamini and Hochberg (1995). Uncertainty in hierarchical clustering was assessed with multiscale bootstrap resampling using approximately unbiased (AU) *p*-values (between 0 and 1) (Suzuki and Shimodeira, 2015). Clusters of the three highest fCO_2-treatments are significantly different at the 0.05 level. Numbers indicate the fCO_2-treatment with average fCO_2 [µatm] between t1-t43.

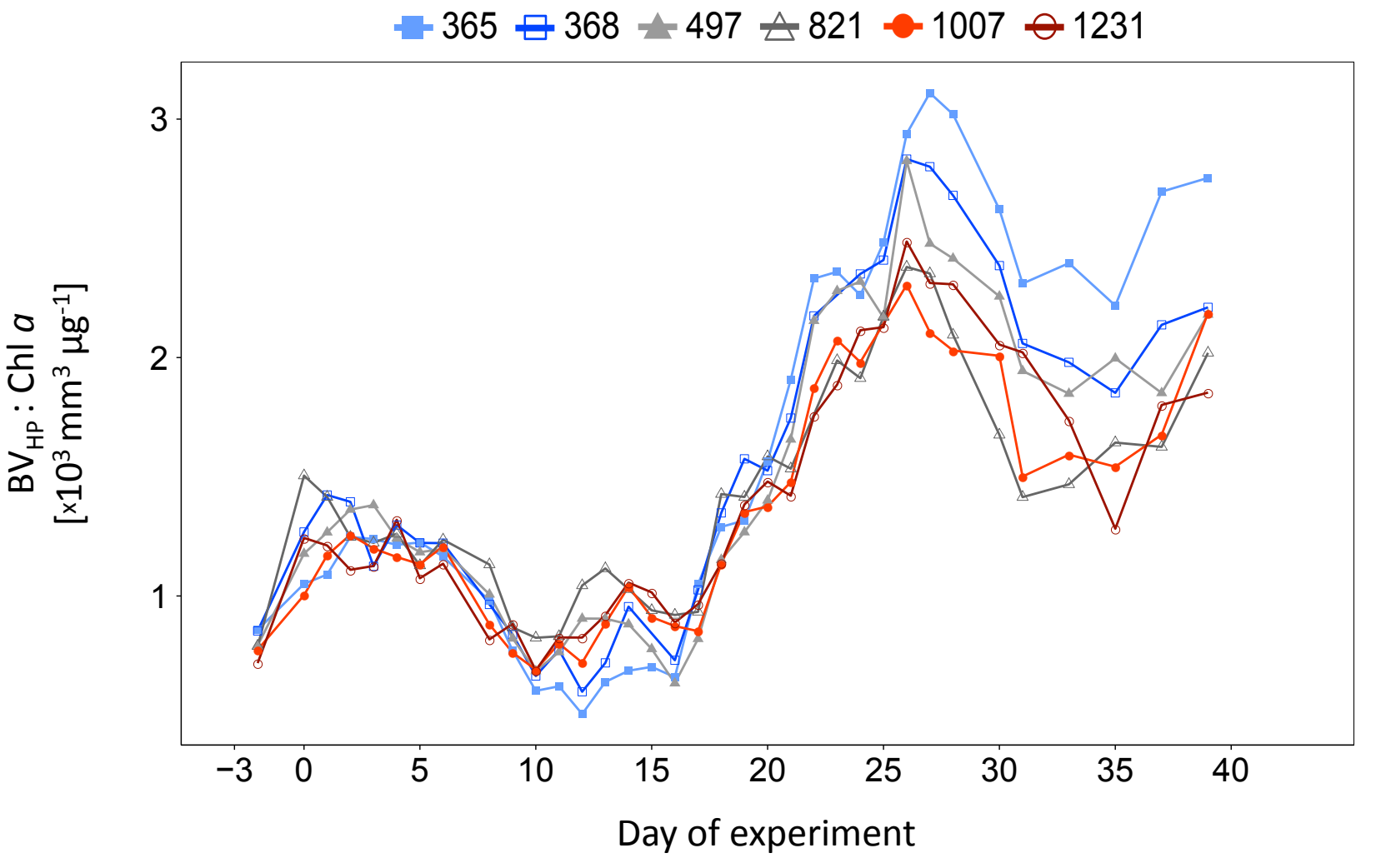
365
368
497
821
1007
1231
3
2
1
BV$_{HP}$: Chl *a*
[x10^3 mm^3 µg^{-1}]
−3
0
5
10
15
20
25
30
35
40
Day of experiment

Figure 5. Standardisation of heterotrophic prokaryotic biovolume to total Chl *a* (BV_{HP} : Chl *a*) during the course of the experiment. PA BV_{HP} was interpolated using splines with software R (R Core Team, 2016) for time-points, where no data were available. Colours and symbols indicate average fCO_2 [µatm] between t1-t43.

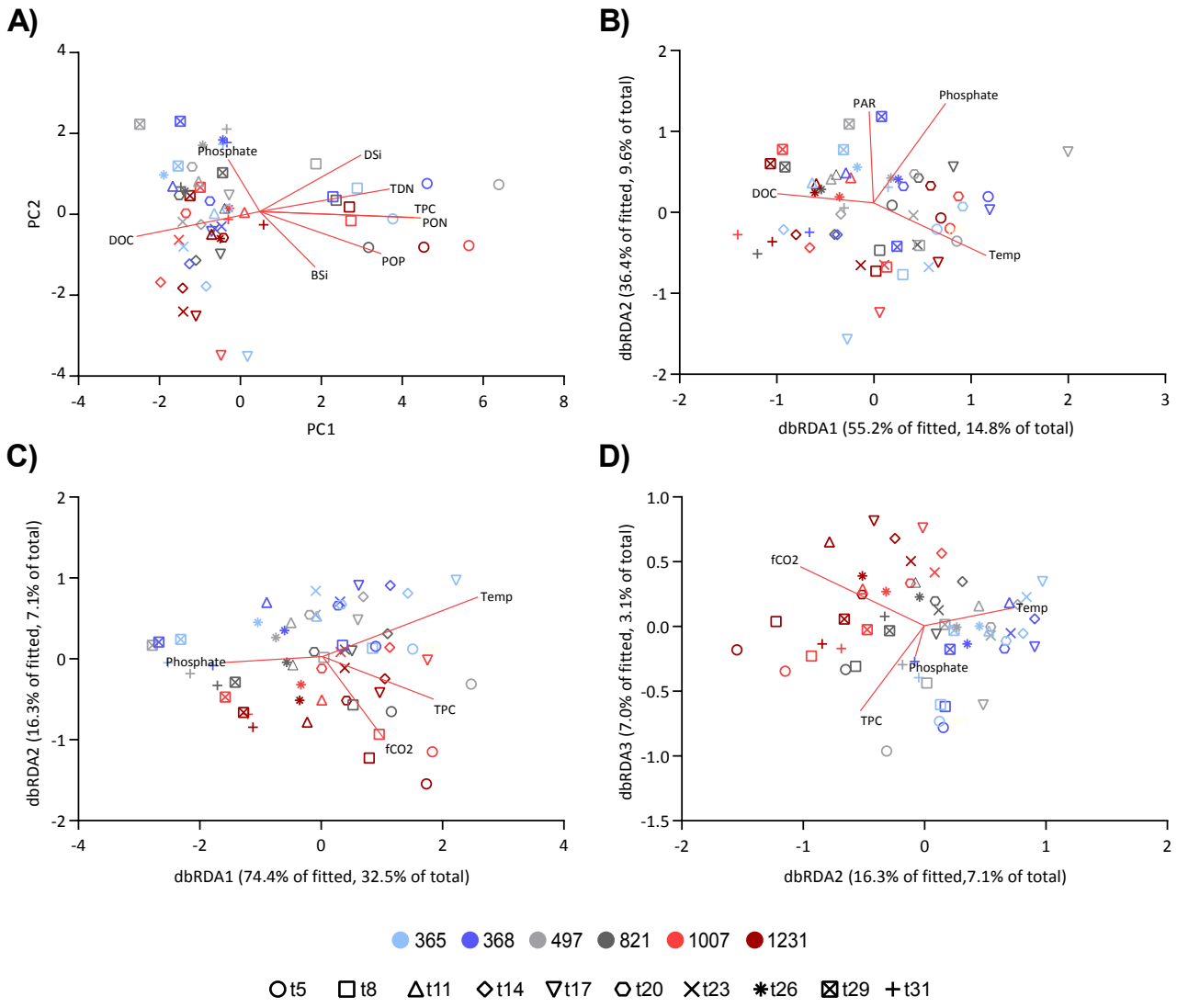
A)
PC2
PC1
Phosphate
DSi
TDN
TPC
PON
POP
BSi
DOC
B)
dbRDA2 (36.4% of fitted, 9.6% of total)
dbRDA1 (55.2% of fitted, 14.8% of total)
PAR
Phosphate
DOC
Temp
C)
dbRDA2 (16.3% of fitted, 7.1% of total)
dbRDA1 (74.4% of fitted, 32.5% of total)
Temp
Phosphate
TPC
fCO2
D)
dbRDA3 (7.0% of fitted, 3.1% of total)
dbRDA2 (16.3% of fitted,7.1% of total)
fCO2
Temp
Phosphate
TPC
365 368 497 821 1007 1231
t5 t8 t11 t14 t17 t20 t23 t26 t29 t31

Figure 6. A) First and second axis of a Principal Component Analysis (PCA) calculated on normalized variables of dissolved and particulate nutrients (n=60). The set of variables and the eigenvectors and –values of the first four axes can be derived from Table 2. B) Ordination of a distance-based redundancy analysis (dbRDA) for visual interpretation of distance-based linear modelling (DistLM) between physical/chemical predictor variables and metabolic variable as well as C-D) abundances of functional bacterial and phytoplankton groups. A Table comprising the set of variables used for DistLM can be derived from the Supplementary (Table S1).